

# Combined effects of polystyrene nanoplastics and lipopolysaccharide on testosterone biosynthesis and inflammation in mouse testis

Yanli Li<sup>a</sup>, Yingqi Liu<sup>a,c</sup>, Yanhong Chen<sup>a</sup>, Chenjuan Yao<sup>b</sup>, Shali Yu<sup>a</sup>, Jianhua Qu<sup>a</sup>, Gang Chen<sup>a,\*</sup>, Haiyan Wei<sup>a,\*</sup>

<sup>a</sup> Department of Occupational Medicine and Environmental Toxicology, College of Public Health, Nantong University, Nantong, Jiangsu 226019, China

<sup>b</sup> Department of Molecular Oral Physiology, Institute of Health Biosciences, University of Tokushima Graduate School, Tokushima-Shi, Tokushima 770-8504, Japan

<sup>c</sup> Wujiang Center for Disease Control and Prevention, Suzhou, Jiangsu 215299, China

## ARTICLE INFO

Handling Editor: Dr Yong Liang

### Keywords:

Nanoplastics  
Lipopolysaccharide  
Testis  
Inflammation  
Testosterone biosynthesis

## ABSTRACT

Microplastics (MPs)/nanoplastics (NPs), as a source and vector of pathogenic bacteria, are widely distributed in the natural environments. Here, we investigated the combined effects of polystyrene NPs (PS-NPs) and lipopolysaccharides (LPS) on testicular function in mice for the first time. 24 male mice were randomly assigned into 4 groups, control, PS-NPs, LPS, and PS-NPs + LPS, respectively. Histological alterations of the testes were observed in mice exposed to PS-NPs, LPS or PS-NPs + LPS. Total sperm count, the levels of testosterone in plasma and testes, the expression levels of steroidogenic acute regulatory (StAR) decreased more remarkable in testes of mice treated with PS-NPs and LPS than the treatment with LPS or PS-NPs alone. Compared with PS-NPs treatment, LPS treatment induced more severe inflammatory response in testes of mice. Moreover, PS-NPs combined with LPS treatment increased the expression of these inflammatory factors more significantly than LPS treatment alone. In addition, PS-NPs or LPS treatment induced oxidative stress in testes of mice, but their combined effect is not significantly different from LPS treatment alone. These results suggest that PS-NPs exacerbate LPS-induced testicular dysfunction. Our results provide new evidence for the threats to male reproductive function induced by both NPs and bacterial infection in human health.

## 1. Introduction

In 1974, Nelson and Bunge first found that the average sperm count and semen volume decreased in normal men (Nelson and Bunge, 1974). In 1992, Carlsen et al. reported that semen quality decreased and sperm count halved in the past 50 years from 1938 to 1991, which attracted global attention (Carlsen et al., 1992). Subsequently, many studies have found a decline in human semen quality and quantity (Akang et al., 2023; Auger et al., 1995; Irvine et al., 1996; Levine et al., 2017). Numerous factors are related to a decline in both the quality and quantity of sperm. Among them, environmental pollutants are considered as an important factor (Okonofua et al., 2022). Epidemiological studies have shown that various environmental pollutants including air pollution, heavy metals, and pesticides can impair human semen quality inducing such as decrease in sperm count, motility, viability, and abnormal morphology (He et al., 2020; Knapke et al., 2022; Manouchehri et al., 2022; Zhou et al., 2014). In vivo studies have elucidated the mechanisms by which environmental contaminants cause damage to

the male reproductive system, such as inhibiting testosterone synthesis, disrupting the blood-testis barrier, inducing inflammation in the testes, and increasing testicular cells apoptosis (Jin et al., 2021; Li et al., 2009; Peretz and Flaws, 2013; Xu et al., 2023).

Microplastics (MPs) and nanoplastics (NPs) are ubiquitous in the natural environment, and they can be found in drinking water, beverages, food, salt, and air (O'Brien et al., 2023; Sewwandi et al., 2023; Zhang et al., 2020). MPs are plastic particles having a diameter of less than five millimeters and NPs are defined as pieces of plastics between one and one hundred nm in diameter. MPs and NPs mostly enter the human body by inhalation or ingestion through the respiratory tract and gastrointestinal tract, respectively (Ramsperger et al., 2023). MPs and NPs are found in human blood (Leslie et al., 2022), saphenous vein tissue (Rotchell et al., 2023), lung tissue (Amato-Lourenco et al., 2021; Jenner et al., 2022), placenta (Ragusa et al., 2021), cirrhotic liver tissue (Horvatis et al., 2022), testis and semen (Montano et al., 2023; Zhao et al., 2023).

Recent investigations have shown that MPs and NPs damage the

\* Corresponding authors.

E-mail addresses: [chengang@ntu.edu.cn](mailto:chengang@ntu.edu.cn) (G. Chen), [why1987@ntu.edu.cn](mailto:why1987@ntu.edu.cn) (H. Wei).

<https://doi.org/10.1016/j.ecoenv.2024.116180>

Received 27 November 2023; Received in revised form 29 February 2024; Accepted 4 March 2024

Available online 8 March 2024

0147-6513/© 2024 The Authors. Published by Elsevier Inc. This is an open access article under the CC BY-NC-ND license (<http://creativecommons.org/licenses/by-nc-nd/4.0/>).

male reproductive functions in mice and rats. Polystyrene microplastics (PS-MPs) and polystyrene nanoplastics (PS-NPs) decrease sperm quality and testosterone level of rodents (Jin et al., 2021; Ilechukwu et al., 2022). In vivo studies have found that MPs and NPs accumulate around the seminiferous tubules (Nikolic et al., 2022) and disrupt the structure of the seminiferous tubules of the mice (Ma et al., 2023). MPs and NPs can be internalized by germ cells, Leydig cells, and Sertoli cells (Jin et al., 2021, 2022) leading to the degeneration and apoptosis of these cells in the testes of mice (Cai et al., 2023; Gao et al., 2023). Subsequently, the increased apoptosis and degeneration of Leydig cells and Sertoli cells lead to a decrease in testosterone levels and disruption of the integrity of the blood-testis barrier (Li et al., 2021; Wei et al., 2021), respectively. Moreover, both in vivo and in vitro studies have found that MPs and NPs inhibit the expression of the steroidogenic acute regulatory (StAR) protein and testosterone synthesis enzymes, such as P450 cholesterol side chain cleavage (P450scc), 3 $\beta$ -hydroxysteroid dehydrogenase (3 $\beta$ -HSD) and 17 $\beta$ -hydroxysteroid dehydrogenase (17 $\beta$ -HSD) (Jin et al., 2022; Sui et al., 2023). Since testosterone and the blood-testis barrier play important roles in the spermatogenesis, damages in Leydig cells and Sertoli cells induced by MPs and NPs indirectly influence spermatogenesis.

About 13–15% of male infertility cases are caused by infection. The most common bacteria that affect semen quality and male fertility are Gram-negative bacteria (Farsimadan and Motamedifar, 2020). Chlamydia trachomatis, a Gram-negative bacterium has been found in the testes, prostate, epididymis, and seminal vesicles (Mackern-Oberti et al., 2013). Gram-negative bacterium has a wall made of bacterial lipopolysaccharide (LPS), which is involved in the pathogenesis of bacterial infections (Alexander and Rietschel, 2001). In animal models, the inflammation caused by LPS can disrupt steroidogenesis and spermatogenesis (Metukuri et al., 2010; Sadasivam et al., 2014).

Bacteria and MPs/NPs are widely present in the natural environment. Multiple studies have shown that MPs/NPs can serve as a vector of pathogenic bacteria in aquatic environments and the pathogenic bacteria attached to MPs/NPs may have various impacts on ecology and human health (Curren and Leong, 2019; Hernández-Sánchez et al., 2023; Junaid et al., 2022). After coexposure to NPs and LPS in mice, NPs exacerbate LPS-induced inflammation in duodenum (He et al., 2022) and spleen (Tang et al., 2022), increasing permeability in duodenum (He et al., 2022), myocardial fibrosis and cardiac autophagy (Lin et al., 2022), apoptosis in kidney (Li et al., 2023) and necroptosis in spleen (Tang et al., 2022). To date, there have been no reports on the combined effects of MPs/NPs and bacterial infections on the male reproductive system. Therefore, it is unknown whether NPs and LPS can synergistically damage the male reproductive system. Here, this study is the first to evaluate the damage of PS-NPs and LPS on mouse testicular function. Overall, our findings suggest that exposure to both PS-NPs and LPS exacerbates the inflammation and reduces testosterone biosynthesis in mice.

2. Materials and methods

2.1. Reagents and antibodies

PS-NPs (Code no: 6–1–0010, size: 0.1  $\mu$ m, microsphere, 2.5% w/v) were purchased from Tianjin Baseline ChromTech Research Centre (Tianjin, China). LPS (L2880) was provided by Sigma-Aldrich Corp. (St. Louis, MO, USA). DMEM/F-12 medium was purchased from Corning Life Sciences (Manassas, VA, USA). Radioimmuno precipitation assay (RIPA) lysis buffer (P0013B), phosphatase inhibitor cocktail A (50  $\times$ ) (P1082), enhanced bicinchoninic acid (BCA) protein assay kit (P0010), lipid peroxidation malondialdehyde (MDA) assay kit (S0131S), reactive oxygen species (ROS) assay kit (S0033S), and total superoxide dismutase assay kit with WST-8 (S0101S), horseradish peroxidase-labeled donkey anti-goat IgG (H + L) (A0181), goat anti-mouse IgG (H + L) (A0216), and goat anti-rabbit IgG (H + L) (A0208) were obtained from Beyotime

Table 1  
Primary antibodies used in western blot analysis.

Antibody	Catalog no.	Corporate brand	Dilution
StAR	sc-166821	Santa Cruz Biotechnology	1:1000
CYP11A1	sc-18043	Santa Cruz Biotechnology	1:1000
IL-1 $\beta$	AF7209	Beyotime Biotechnology	1:2000
IL-6	AF7236	Beyotime Biotechnology	1:2000
MCP1	ab7202	Abcam	1:2000
TNF- $\alpha$	sc-52746	Santa Cruz Biotechnology	1:1000
Phospho-NF- $\kappa$ B p65	3033 s	Cell Signaling Technology	1:1000
NF- $\kappa$ B p65	8242 s	Cell Signaling Technology	1:1000
phospho-I $\kappa$ B $\alpha$	AF5851	Beyotime Biotechnology	1:1000
$\beta$ -actin	A3854	Sigma-Aldrich	1:20000

Table 2  
The sequences of primers used in the study.

Gene	Forward primer (5'-3')	Reverse primer (5'-3')
StAR	CACTCTATAGTGACCAGGAG	CAGGACCTTGATCTCCTTGA
CYP11A1	CAGATGCCTGGAAGAAAGAC	GACAGCAATTGATGAACCGCT
IL-1 $\beta$	CTTCAGGCAGGCAGTATCA	TGTCCATTGAGGTGGAGAG
IL-6	TAGTCCTTCTACCCCAATTTC	TTGGTCCTTAGCCACTCCTTC
MCP1	GCTGCTACTCATTCACCA	TGGACCCATTCTCTCTTG
TNF- $\alpha$	GACGTGGAAGTGGCAGAAGAG	TTGGTGGTTTGTGAGTGTGAG
GAPDH	ATGGGAAGCTGGTCATCAAC	TGTGAGGGAGATGCTCAGTG

Biotechnology (Shanghai, China). The complete protease inhibitor cocktail tablet was provided by Roche Applied Sciences (Indianapolis, IN, USA). Immobilon-P polyvinylidene difluoride membrane and the enhanced chemiluminescence (ECL) detection kit were obtained from Merck Millipore (Merck KGaA, Darmstadt, Germany). RNAiso Plus, PCR amplification kit, and Primescript II RT enzyme kit were produced by Takara Biotechnology (Dalian, Liaoning, China). The mouse testosterone ELISA kit (E-OSEL-M0003) was obtained from Elabscience Biotechnology Co. Ltd (Wuhan, Hubei, China). The primary antibodies and the sequences of primers used in this study are listed in Table 1 and Table 2, respectively.

2.2. Characterization of PS-NPs

The morphological characteristics of PS-NPs were determined by a scanning electron microscope (SEM, ZEISS, GeminiSEM 300, Germany). The PS-NPs were diluted with pure water at a concentration of 50  $\mu$ g/mL. One drop of the PS-NPs suspension was fixed on a 200-mesh copper grid and air dry. PS-NPs were coated with a thin layer of gold and palladium for 2 min and measured at 5 kV. The particle size was measured from the SEM images using Image J 1.47 v software (<http://imagej.nih.gov/ij>). The chemical composition of NPs was determined by Fourier Transformed Infrared Spectroscopy (FTIR, Nicolet IS 10, Thermo Fisher Scientific, USA). 1 mL of NPs solution used in this study was dried at 35  $^{\circ}$ C in a dry condition. FTIR spectra were acquired using a Nicolet Summit FTIR equipped with an Everest ATR with a diamond Crystal plate and a DTGS KBr detector.

2.3. Animals and treatment

6–8-week-old SPF ICR male mice were obtained from the Experimental Animal Center of Nantong University. The mice were kept in an environment with temperature of 22  $\pm$  2  $^{\circ}$ C, relative humidity 70%, and 12 h light-dark cycle. All animal experiments in this study were approved by the Ethics Committee for Experimental Animal Care and Welfare of Nantong University (Permission number: S20231030–001). The mice used in this study were observed for three days before the experiment, and the healthy mice were used in the following research. The mice were randomly assigned into four groups (6 mice in each group), control group, PS-NPs group, LPS group, and PS-NPs + LPS group. Mice in the PS-NPs group and the PS-NPs + LPS group received

intraperitoneal injection with 30 mg/kg/day of PS-NPs for four consecutive days. This dose of PS-NPs was selected because the data published by Senathirajah K. Senathirajah et al. showed that the estimated average weekly exposure dose of human MPs was 0.1–5 g (Senathirajah et al., 2021). In order to study the harmful effects of MPs at lower doses, we took the weekly exposure dose of 1.5 g, calculated according to the per capita weight of 60 kg, and considered the equivalent dose ratio of humans and animals. 12 h before the experimental observation endpoint, mice in the LPS group and the PS-NPs + LPS group were intraperitoneally administered with 5 mg/kg of LPS (Rokade et al., 2021) which was reported to induce systemic inflammation in male mice. The control group was intraperitoneally injected with the same volume of 0.9% saline daily. On the fifth day, the mice were sacrificed, and testicular tissue and whole blood were collected.

#### 2.4. Hematoxylin-Eosin (H & E) staining

For testicular histology, one intact testis of the mouse was fixed with animal testicular tissue fixative, and the testicular tissue capsule was pierced with a needle to ensure complete infiltration of the fixative into the tissue. After fixation at room temperature for 24 h, the testis was transferred to 70% ethanol for dehydration. Paraffin embedding was performed, and 4  $\mu$ m sections were stained with H & E. Images were captured using digital pathological section scanner KF-PRO-005-EX (Ningbo, Zhejiang, China). Damage to the seminiferous tubules was determined by measuring seminiferous tubules thickness and lumen area (Sziva et al., 2022). At least 10 seminiferous tubules were randomly selected and detected from sections of testicular tissue in each group. The areas of seminiferous tubules and lumen were calculated by K-Viewer 1.7.1.1 software (<https://www.kfbio.cn/k-viewer/>), and the ratio of lumen area to seminiferous tubules area was expressed as a percentage. The average spermatogenic epithelium of the seminiferous tubules were measured by K-Viewer 1.7.1.1 software and calculated in  $\mu$ m.

#### 2.5. Total sperm count

Left epididymis was taken from each mouse for sperm counting. The epididymis was gently cut into small pieces in 1 mL phosphate-buffered saline (PBS) and incubated at 37 °C with 5% CO<sub>2</sub> for 20 min to release the sperm into the PBS buffer. Sperm count was determined by a hemocytometer under a light microscope. As this method is subjective, the evaluation of sperm count in each epididymis was conducted by three independent researchers, ultimately taking the average of these three counts.

#### 2.6. Evaluation of testicular reactive oxygen species (ROS)

The level of oxidative stress in testicular tissue of mice was detected by ROS detection kit. The fresh testicular tissue (20 mg) was isolated capsule and cut into small pieces in 0.5 mL serum-free DMEM/F-12 medium. The testicular tissue was gently crushed with a grinding pestle and repeatedly pipetted to disperse cells. The lysate was centrifuged at 100 rpm for 1 min to remove a small amount of tissue that was not completely broken, and the supernatant was transferred to a new tube using a pipette and centrifuged at 1000 rpm for 5 min. The cells were resuspended in DMEM/F-12 medium containing DCFH-DA (1:1000) without serum and incubated at 37 °C for 20 min and then washed with serum-free DMEM/F-12 medium for three times. The cells were transferred to a 24-well plate and the fluorescence intensity was detected using a fluorescence microplate reader (Infinite E Plex, Tecan, Gradišch, Austria) with an excitation wavelength at 488 nm. The results showed as relative values between the treatment group and the control group.

#### 2.7. Testicular MDA content assay

20 mg testicular tissue was mixed with lysis buffer (1:9 wt volume ratio) containing. The lysate was centrifuged at 12,000 rpm for 10 min at 4 °C. The supernatant was used for the following assays. The protein concentration was detected by BCA protein assay, and the MDA content in the sample was detected by thiobarbiturate (TBA) method. Briefly, 0.1 mL lysate and 0.2 mL 0.1% TBA solution were mixed and incubated at 100 °C for 15 min, and then centrifuge at 1000 rpm for 10 min at room temperature. The supernatant (200  $\mu$ L) was added to 96-well plates, and the absorbance was determined with a microplate reader (Infinite E Plex, Tecan, Gradišch, Austria) at wavelength 532 nm. The MDA content was calculated by the protein content per unit weight.

#### 2.8. Measurement of testicular SOD activity assay

To measure the testicular SOD activity, 10 mg testicular tissue was added with 100  $\mu$ L lysis buffer. The homogenate was centrifuged at 12000 rpm at 4 °C for 5 min. The protein concentration of supernatant was measured by BCA protein assay. The activity of SOD was measured by WST-8 assay. Briefly, testicular sample and WST-8 solution were incubated at 37 °C for 30 min, then the absorbance of the sample was determined by a microplate reader (BioTek ELX800, BioTek Instruments Inc. USA) at wavelength 450 nm. The results were calculated by the protein content per unit weight.

#### 2.9. Detection of testosterone concentration in plasma and testes by ELISA

Blood was collected in a 2 mL anticoagulant tube and held at room temperature for 2 h and then centrifuged for 20 min at 1000 rpm. The plasma was used for testosterone measurement. The right testicular tissue was cut into pieces and mixed with 1  $\times$  PBS containing protease inhibitor cocktail (1:9 wt volume ratio). The homogenate was centrifuged at 5000 rpm for 10 min at 4 °C, and the supernatant was used for detecting testosterone concentration. Testosterone levels in plasma and testes of mice were evaluated using ELISA kits according to the manufacturer's procedures. Briefly, 50  $\mu$ L plasma or tissue homogenate was added to each well of a 96-well ELISA plate, followed by the addition of 50  $\mu$ L peroxidase-coupled immunoglobulin G anti-testosterone to each well. The plate was then incubated for 1 h at 37 °C. After rinsing the plate with washing buffer 5 times, 90  $\mu$ L of substrate solution was added to each well and incubated at 37 °C for 15 min. The reaction was terminated by adding 50  $\mu$ L of termination solution to each well. Finally, the absorbance of testosterone was measured by a microplate reader (BioTek ELX800, BioTek Instruments Inc. USA) at wavelength 450 nm. The results were expressed as the ratio of testosterone to testicular tissue protein content of sample.

#### 2.10. Total RNA extraction and semi-quantitative reverse transcription (RT)-PCR

Total RNA of mouse testes was extracted using RNAiso Plus reagent according to the manufacturer's instructions. 2.5  $\mu$ g of total RNA as a template was reverse transcribed into cDNA using the Prime Script II RT kit. A 20  $\mu$ L PCR reaction was then performed using 1.0  $\mu$ L of cDNA as a template for semi-quantitative PCR amplification. The PCR reaction conditions consisted of an initial denaturation at 95 °C for 5 min, followed by 20–25 cycles of denaturation at 95 °C for 30 s, annealing at the appropriate temperature for 30 s, and extension at 72 °C for 1 min. The final cycle was followed by extension at 72 °C for 10 min and cooling at 4 °C. The PCR product was electrophoresed on a 2.5% agarose gel and then stained by 0.5  $\mu$ g/mL ethidium bromide. The DNA was visualized under ultraviolet light using a Bio-Rad Gel Doc TM EZ imager, and the gel bands were analyzed using Image J 1.47 v software (<http://imagej.nih.gov/ij/>).

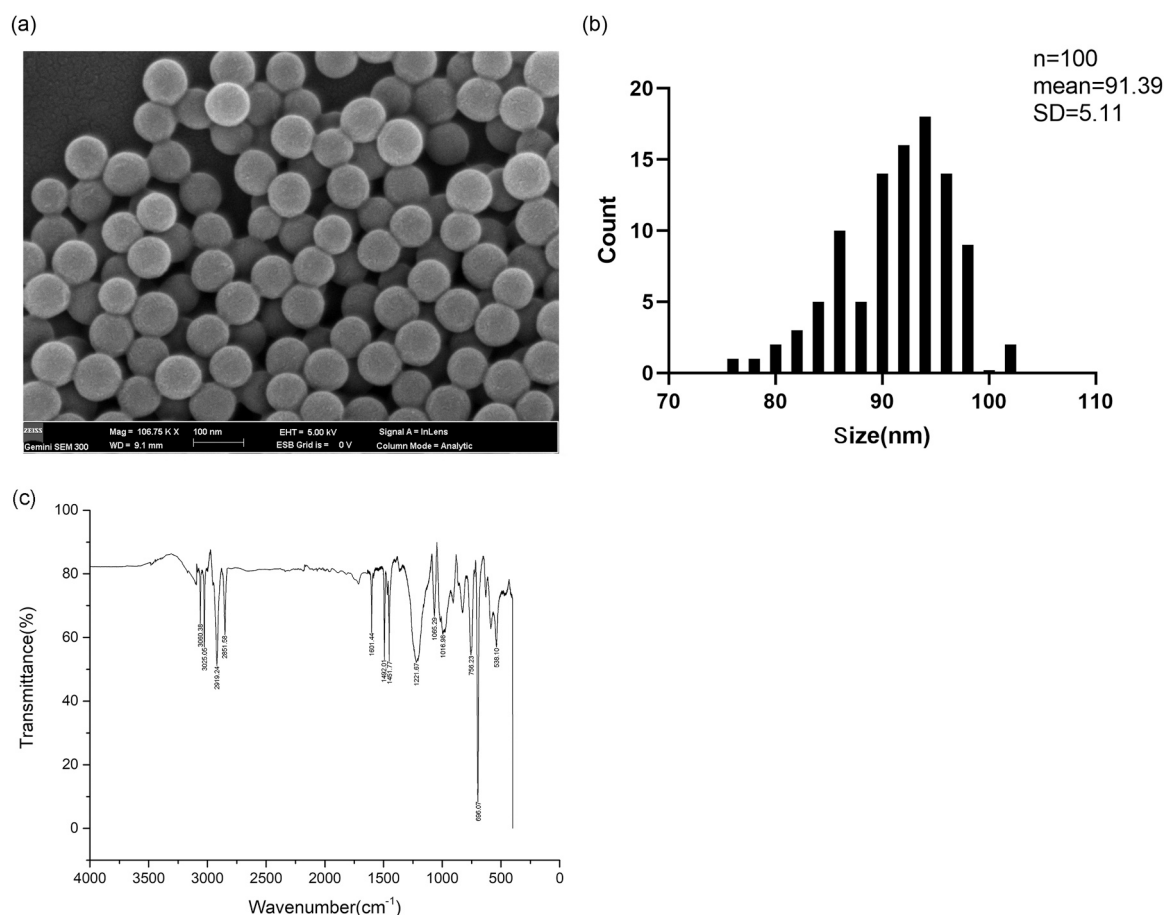


**Fig. 1.** Characteristics of PS-NPs. (a) Image of PS-NPs by scanning electron microscope (SEM). Scale bars, 100 nm; (b) The size distribution of 100 PS-NPs was attained from SEM image using Image J software. (c) The component of NPs was measured by FTIR spectrum.

### 2.11. Protein extraction and Western blot analysis

A protease inhibitor cocktail was added to ice-cold RIPA buffer, which was used to homogenize the mouse testicular tissue. The homogenate was centrifuged at 12,000 rpm for 15 min at 4 °C, and the supernatant was used as a protein sample. The protein concentration of the supernatant was quantified using a BCA protein assay. The samples were then denatured at 95 °C for 5 min in the water bath. 20 µg (for target protein) or 10 µg (for β-actin) of protein per lane was separated on a 10% SDS-polyacrylamide gel at 80 mV for 2 h. Wet transfer membrane was performed at a constant current of 300 mA. The membrane was blocked with 0.1% Tween-20 in 1 × Tris-buffered saline (TBS-T) containing 5% skim milk (for non-phosphorylated antibody) or 4% BSA (for phosphorylated antibody) at room temperature for 2 h, then the membrane was incubated with specific primary antibody at 4 °C overnight. The membrane was washed with TBS-T and incubated with goat anti-rabbit or mouse and donkey anti-goat IgG at room temperature for 1 h. Proteins were determined using ECL immunoblotting substrates, and images were captured using the Tanon 5500 imaging chemiluminescence system (Tanon, Shanghai, China). The target proteins were compared with the internal reference protein (β-actin). Bands were analyzed using grayscale analysis with Image J 1.47 v software (<http://imagej.nih.gov/ij>).

### 2.12. Statistical analysis

Each experiment consisted of 5–6 biological replicates. The experimental results were reported as the mean ± standard deviation (SD). The Kolmogorov-Smirnov test was employed to assess normality, while

Levene's test was used to examine homogeneity of variance. For comparing data among multiple groups, one-way ANOVA and Tukey's HSD post hoc test were applied. Statistical significance was determined when the p-value was less than 0.05.

## 3. Results

### 3.1. Characteristics of PS-NPs

As shown in Fig. 1a, the PS-NPs used in this study exhibited spherical morphology, uniform size, and shape. The size of 100 PS-NPs was analyzed using Image J 1.47 v software, the average diameter of mono dispersed PS-NPs was about 91.39 nm (Fig. 1b). FTIR spectrum of NPs used in this study was presented in Fig. 1c. The sharp peaks at 3060.38 and 3025.05 cm<sup>-1</sup> were due to the aromatic C - H stretching, while the sharp peaks at 1601.44, 1492.01, 1451.77 cm<sup>-1</sup> were due to the C = C aromatic stretching. The absorption peaks at 2919.24 and 2851.58 cm<sup>-1</sup> corresponded to the presence of methylene. The absorption peaks at 756.23 and 696.07 cm<sup>-1</sup> corresponded to C - H out-of-plane bending vibration absorption and indicating that there was only one substituent in the benzene ring. FTIR analysis indicated that the component of NPs used in this study was polystyrene.

### 3.2. The combined effect of PS-NPs and LPS on testicular histology and total sperm count in mice

H & E staining showed that the ratio of seminiferous tubule lumen area to total seminiferous tubule area in the control group, PS-NPs group, LPS group, and LPS+PS-NPs group was 7.87%, 8.94%, 17.41%,

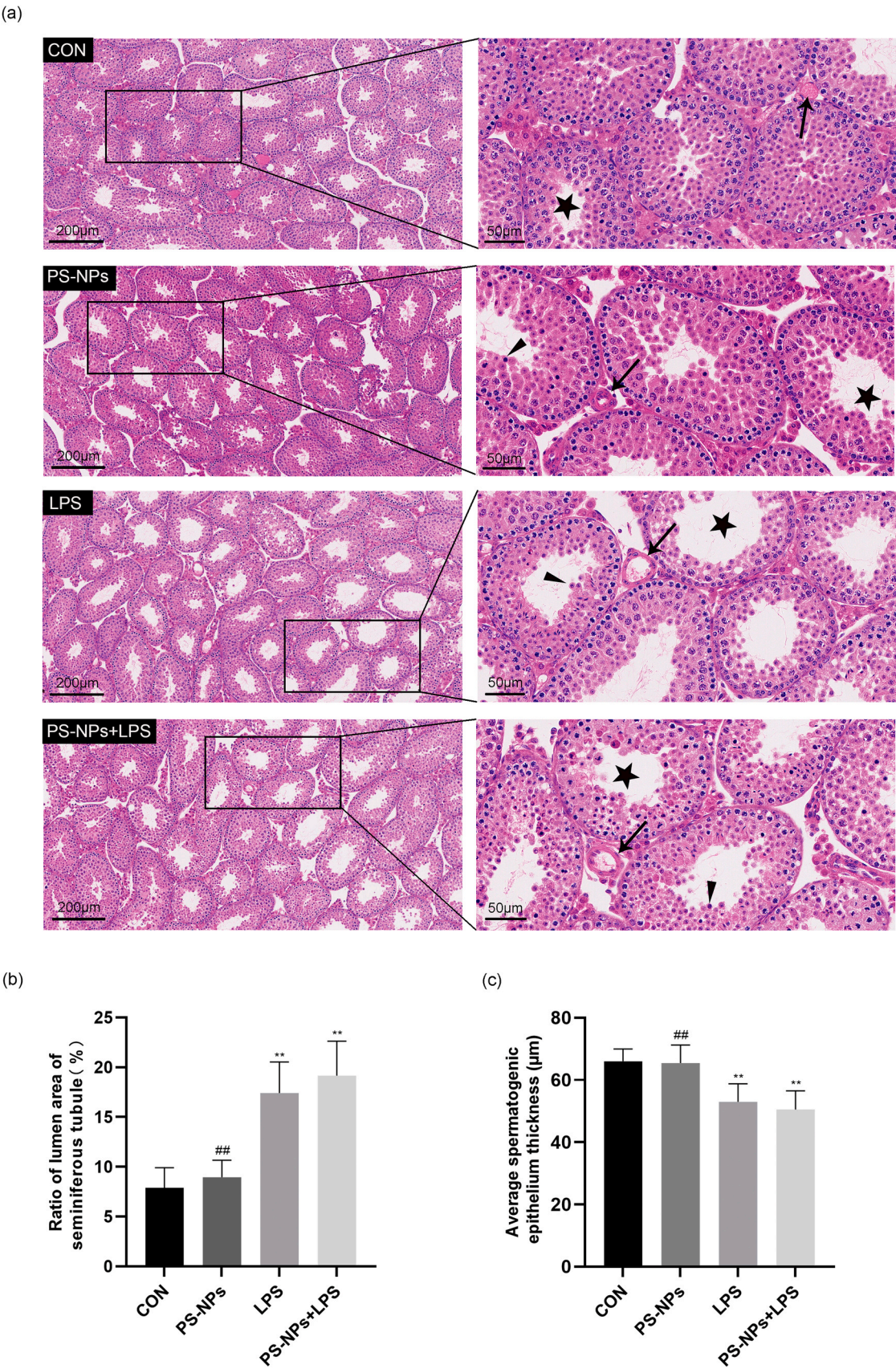


**Fig. 2.** The combined effect of PS-NPs and LPS on testicular histology and total sperm count in mice. H & E staining of testis (a), the ratio of lumen area to seminiferous tubules area (b), the average spermatogenic epithelium of the seminiferous tubules (c) in the control, PS-NPs, LPS and PS-NPs + LPS group. Arrows indicate blood vessels, and asterisks indicate seminiferous tubules lumen. Results were presented as the mean  $\pm$  SD ( $n = 6$ ). <sup>\*\*</sup>  $p < 0.01$  vs the control group. <sup>##</sup>  $p < 0.01$  vs the PS-NPs + LPS group.

**Table 3**

The combined effect of PS-NPs and LPS on the sperm count of male mice.

Group	Sperm count (10 <sup>6</sup> sperm/epididymis)
Control	57.99 ± 6.15
PS-NPs	41.43 ± 4.28 <sup>***</sup>
LPS	26.54 ± 4.66 <sup>***</sup>
PS-NPs + LPS	19.38 ± 3.54 <sup>**</sup>

Values were presented as mean ± SD (n = 6). <sup>\*\*</sup> p < 0.01 vs the control group.<sup>\*\*\*</sup> p < 0.01 vs PS-NPs + LPS group.**Table 4**

The combined effects of PS-NPs and LPS on ROS, MDA, and SOD in testes of male mice.

Group	ROS relative level	MDA (nmol / mg protein )	SOD (unit / mg protein)
Control	1.00 ± 0.10	0.58 ± 0.11	117.68 ± 7.99
PS-NPs	1.82 ± 0.10 <sup>***</sup>	1.02 ± 0.19 <sup>***</sup>	107.25 ± 2.86 <sup>##</sup>
LPS	2.54 ± 0.37 <sup>**</sup>	1.86 ± 0.14 <sup>**</sup>	74.37 ± 8.70 <sup>**</sup>
PS-NPs + LPS	2.66 ± 0.36 <sup>**</sup>	1.88 ± 0.08 <sup>**</sup>	63.06 ± 10.66 <sup>**</sup>

Values were presented as mean ± SD (n = 5). <sup>\*\*</sup> p < 0.01 vs the control group.<sup>##</sup> p < 0.01 vs PS-NPs + LPS group.

and 19.16%, respectively (Fig. 2a and b). The thickness of the seminiferous epithelium in the corresponding group was 66.00, 65.44, 52.94, and 50.53  $\mu$ m, respectively (Fig. 2a and c). Enlargement of the seminiferous tubule lumen area (Fig. 2a and b) and reduced thickness of spermatogenic epithelium (Fig. 2a and c) were observed in the LPS and PS-NPs + LPS groups, but were not observed in the control and PS-NPs group. The blood vessels of interstitial tissues in the control group were filled with erythrocytes, while blood cells exuded from vessels and the blood vessel walls swelled in the PS-NPs, LPS and PS-NPs + LPS groups (Fig. 2a). Compared with the control group, mice exposed to PS-NPs or LPS alone showed a decreased sperm count per epididymis from 57.99 million to 41.43 million or 26.54 million, respectively. After coexposure to PS-NPs and LPS, sperm count per epididymis in mice decreased to 19.38 million with a significant statistical difference compared to the PS-NPs or LPS group (Table 3).

### 3.3. The combined effect of PS-NPs and LPS on oxidative stress in testes of mice

Next, we measured the oxidative stress and the antioxidant level in the testes of mice exposed to PS-NPs, LPS, and PS-NPs + LPS in vivo. Compared with the control group, the production of ROS in the testes of mice in PS-NPs, LPS, and PS-NPs + LPS groups increased by 1.8-, 2.5-, and 2.7-fold, respectively (Table 4). However, there was no significant difference between the PS-NPs + LPS group and the LPS group ( $P \geq 0.05$ ) (Table 4). The MDA levels in the testes of mice in the control group, PS-NPs, LPS, and PS-NPs + LPS group were 0.58, 1.02, 1.86, and 1.88 nmol/mg protein, respectively. Compared with the control group, there was a statistically significant difference in MDA level in the testes of each treatment group ( $P < 0.01$ ) (Table 4). Similar to the changes on ROS, there was no difference in the MDA level of testes between the PS-NPs + LPS group and the LPS group ( $P \geq 0.05$ ) (Table 4). The antioxidant activity of SOD level in the testes of mice in the control group, PS-NPs, LPS, and PS-NPs + LPS group were 117.7, 107.3, 74.4, and 63.1 unit/mg protein, respectively (Table 4). Exposure to LPS alone or with PS-NPs, induced a remarkable decrease in SOD as compared to that of control group (Table 4). However, exposure to PS-NPs alone did not inhibit the activity of SOD (Table 4). These findings indicate that exposure to PS-NPs or LPS alone can induce oxidative stress, but their combined effect on oxidative stress does not exceed that of exposure to LPS alone.

**Table 5**

The combined effect of PS-NPs and LPS on testosterone levels in plasma and testes of male mice.

Group	Plasma (ng / mL)	Testicular tissue (ng / g protein)
Control	4.83 ± 1.45	266.20 ± 90.11
PS-NPs	0.80 ± 0.08 <sup>***</sup>	108.32 ± 6.25 <sup>***</sup>
LPS	0.51 ± 0.06 <sup>**</sup>	54.62 ± 18.73 <sup>**</sup>
PS-NPs + LPS	0.33 ± 0.03 <sup>**</sup>	40.08 ± 10.35 <sup>**</sup>

Values were presented as mean ± SD (n = 5). <sup>\*\*</sup> p < 0.01 vs. the control group.<sup>##</sup> p < 0.05 vs PS-NPs + LPS group. <sup>\*\*\*</sup> p < 0.01 vs PS-NPs + LPS group.

### 3.4. The combined effect of PS-NPs and LPS on testosterone levels and expression of key genes in testosterone biosynthesis in mice

Testosterone is essential for maintaining spermatogenesis and male fertility. The plasma testosterone levels in the control group, PS-NPs, LPS, and PS-NPs + LPS group were 4.83, 0.80, 0.51, and 0.33 ng/mL, respectively. The testosterone levels in the testes of mice in corresponding group were 266.20, 108.32, 54.62, and 40.08 ng/g protein, respectively (Table 5). Compared with the control group, treatment with PS-NPs or LPS induced a dramatic decrease in plasma ( $P < 0.01$ ) (Table 5) and testicular ( $P < 0.01$ ) (Table 5) testosterone levels. PS-NPs combined with LPS significantly decreased the levels of plasma testosterone and testicular testosterone compared with exposure to LPS ( $P < 0.05$ ) or PS-NPs alone ( $P < 0.01$ ) (Table 5). Next, we detected the expression of two key genes involved in testosterone biosynthesis. Surprisingly, StAR mRNA (Fig. 3a) and protein (Fig. 3b) expression in mouse testes were significantly reduced by LPS or PS-NPs treatment, but the decrease induced by PS-NPs was weaker than that of LPS. PS-NPs combined with LPS exposure resulted in lower levels of StAR mRNA and protein in mouse testes compared to the LPS-treated group alone (Fig. 3a and b). Compared with the control group, treatment with LPS, but not PS-NPs, affected the expression levels of CYP11A1 mRNA and protein in the testes of mice. The expression levels of CYP11A1 mRNA and protein were significantly lower in PS-NPs combined with LPS treatment group compared to LPS treatment group alone (Fig. 3a and b). These findings suggest that PS-NPs combined with LPS inhibit StAR and CYP11A1 expression which results in a decrease in testosterone levels in the testes and plasma.

### 3.5. The combined effect of PS-NPs and LPS on inflammatory factors expression in testes of mice

Inflammation is an important factor leading to testicular dysfunction. Next, we investigated the effects of PS-NPs, LPS, and the combined treatment of PS-NPs and LPS on the expression levels of inflammatory factors in testes of mice. Compared with the control group, the expression levels of interleukin-1 beta (IL-1 $\beta$ ), interleukin-6 (IL-6), monocyte chemoattractant protein 1 (MCP1) and tumor necrosis factor alpha (TNF- $\alpha$ ) mRNA and protein in mouse testes were significantly increased in the LPS treated group, while they were slightly increased in the PS-NPs-treated group (Fig. 4a and b). Compared with the LPS-treated group, the expression levels of IL-1 $\beta$ , IL-6, MCP1, and TNF- $\alpha$  mRNA and protein in mouse testes significantly increased in the PS-NPs + LPS treated group (Fig. 4a and b). These results indicate that PS-NPs significantly exacerbate LPS-induced inflammation in testes.

Next, we detected NF- $\kappa$ B phosphorylation level in the testes of mice. Treatment with LPS alone and combined with PS-NPs induced a significantly increase in the phosphorylation level of NF- $\kappa$ B in testes of mice compared with the control group (Fig. 4c). NF- $\kappa$ B activation requires the phosphorylation and degradation of inhibitory kappa B (I $\kappa$ B) proteins. In addition, we detected the phosphorylation level of I $\kappa$ B  $\alpha$ . Compared with the control group, the phosphorylation level of I $\kappa$ B  $\alpha$  was significantly increased in the testes of the PS-NPs group alone, the LPS group alone, and the PS-NPs combined with LPS group. The testicular I $\kappa$ B  $\alpha$

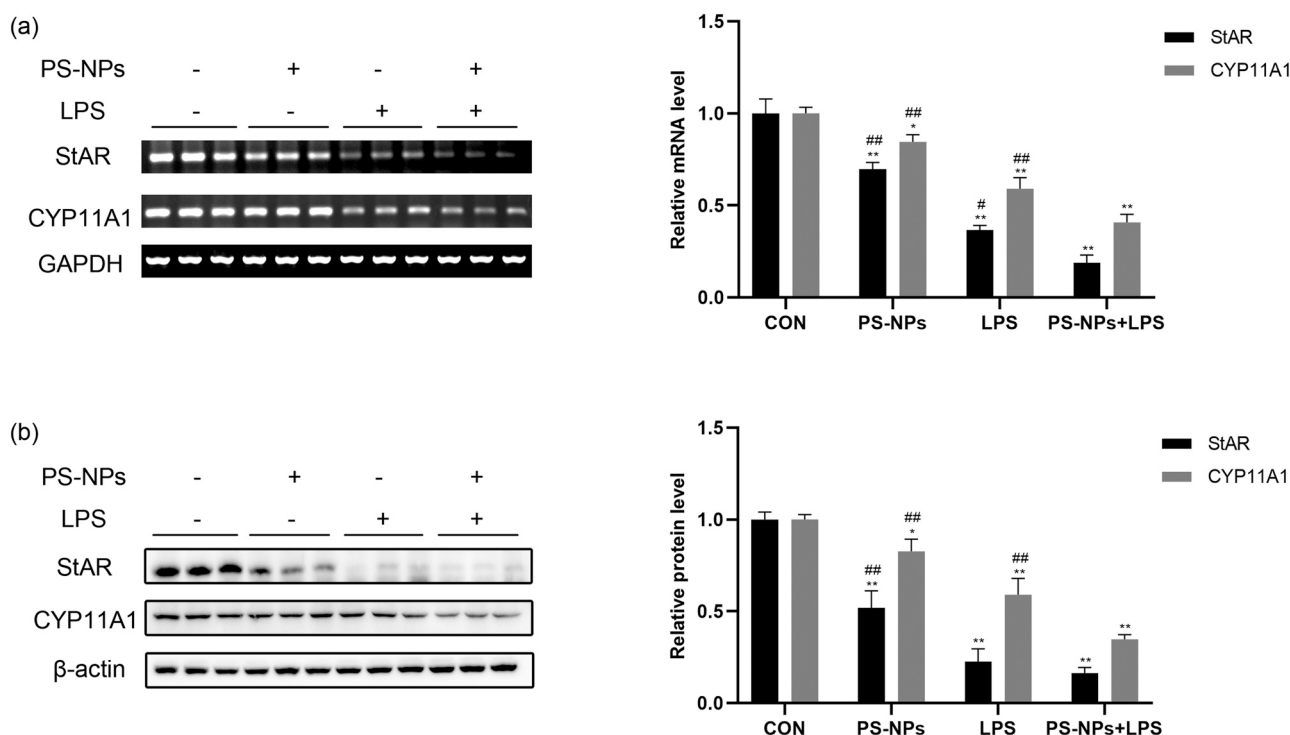


**Fig. 3.** The combined effect of PS-NPs and LPS on expression of key genes in testosterone biosynthesis in mice. (a) The mRNA expressions of StAR and CYP11A1 in testicular tissue of mice in the control, PS-NPs, LPS and PS-NPs + LPS group were detected by Semi-quantitative RT-PCR. GAPDH serves as an internal control for mRNA. The bar chart summarized the expression levels of StAR and CYP11A1 mRNA in the PS-NPs, LPS, and PS-NPs + LPS group normalized to the control group. (b) The protein expressions of StAR and CYP11A1 in testicular tissue of mice in the control, PS-NPs, LPS and PS-NPs + LPS group were detected by Western blot analysis.  $\beta$ -actin serves as an internal control for protein. The bar chart summarized the expression levels of StAR and CYP11A1 protein in the PS-NPs, LPS, and PS-NPs + LPS group normalized to the control group. Results were presented as the mean  $\pm$  SD ( $n = 6$ ). \* $p < 0.05$  and \*\* $p < 0.01$  vs the control group. # $p < 0.05$  and ## $p < 0.01$  vs the PS-NPs or LPS group compared to the PS-NPs + LPS group.

phosphorylation levels in the PS-NPs combined with LPS treatment group were significantly higher than those in the LPS treatment group alone (Fig. 4c). These results suggest that the combination of PS-NPs and LPS significantly enhances the activity of NF- $\kappa$ B in testes.

#### 4. Discussion

Gram-negative bacteria are the most common pathogen of orchitis and epididymitis (Ryan et al., 2018). In vivo studies have shown that MPs and NPs can accumulate in the testes of rodents and damage their reproductive function (Hassine et al., 2023). Moreover, MPs can be detected in human testes (Zhao et al., 2023). MPs/NPs are believed to accumulate pathogenic bacteria and act as a vector of pathogenic bacteria, while pathogenic bacteria through MPs/NPs can cause various damages on ecology and human health (Junaid et al., 2022). We evaluated the combined effects of PS-NPs and LPS on testosterone biosynthesis and inflammation in the testes of mice in this study. Our results indicated that combined exposure to LPS and PS-NPs significantly increased inflammation and reduced testosterone biosynthesis in the testes of mice. To our knowledge, this is the first study to elucidate the combined effect of PS-NPs and LPS on the rodent testes.

In this study, short-term exposure to PS-NPs mainly affected testicular interstitial tissue, such as increased interstitial space, swelled vascular walls, and leakage of cells from the blood vessels. This change is consistent with the increase in inflammation induced by PS-NPs. The inflammatory response of testicular interstitial tissue induced by PS-NPs may play an important role in reducing the synthesis of testosterone by Leydig cells. Testosterone is required for at least three critical processes during spermatogenesis: maintenance of the blood-testis barrier, meiosis, and sperm release (Smith and Walker, 2014). The combined exposure to LPS and PS-NPs significantly reduced the level of

testosterone which could be the main influencing factor for the decrease in sperm count. Short-term exposure to PS-NPs did not cause any damage to the epithelial thickness and lumen area of the seminiferous tubules, and no differences were observed in the damage of the seminiferous tubules induced by the combination of LPS and PS-NPs compared to LPS alone.

Compared with exposure to LPS or PS-NPs, combined exposure to LPS and PS-NPs significantly inhibited the mRNA and protein levels of important genes including StAR and CYP11A1, which were involved in testosterone synthesis in the testes of mice. Correspondingly, combined exposure to LPS and PS-NPs significantly reduced testosterone levels in mouse plasma and testicular tissue. StAR permits translocation of cholesterol from the outer to the inner mitochondrial membrane for initiation of testosterone synthesis and governs the rate-limiting step in steroidogenesis in Leydig cells of testes. Acute exposure to LPS inhibits StAR expression and disrupts steroidogenesis (Allen et al., 2004; Bosmann et al., 1996; Shen et al., 2022). Short term treatment with PS-MPs or PS-NPs in mice also inhibits StAR expression, and multiple studies have demonstrated the molecular mechanism by which PS-MPs or PS-NPs decrease StAR expression and reduce testosterone levels in vivo (Sui et al., 2023) and in vitro (Sun et al., 2023). Our findings indicated that combined exposure to PS-NPs and LPS resulted in a devastating decrease in the expression levels of StAR mRNA and protein, which were worse than those induced by LPS or PS-NPs alone. Our previously published paper indicates that PS-NPs inhibit the mRNA and protein levels of StAR by increasing hypoxia-inducible factor-1 $\alpha$  (HIF-1 $\alpha$ ) expression (Sui et al., 2023). LPS enhances the transcription level of HIF-1 $\alpha$  by binding activated NF- $\kappa$ B to the HIF-1 $\alpha$  promoter (Frede et al., 2006). LPS also increases HIF-1 $\alpha$  mRNA expression in rat testes (Palladino et al., 2018). The results of this study indicate that, compared to exposure to LPS or PS-NPs, combined exposure to LPS and PS-NPs

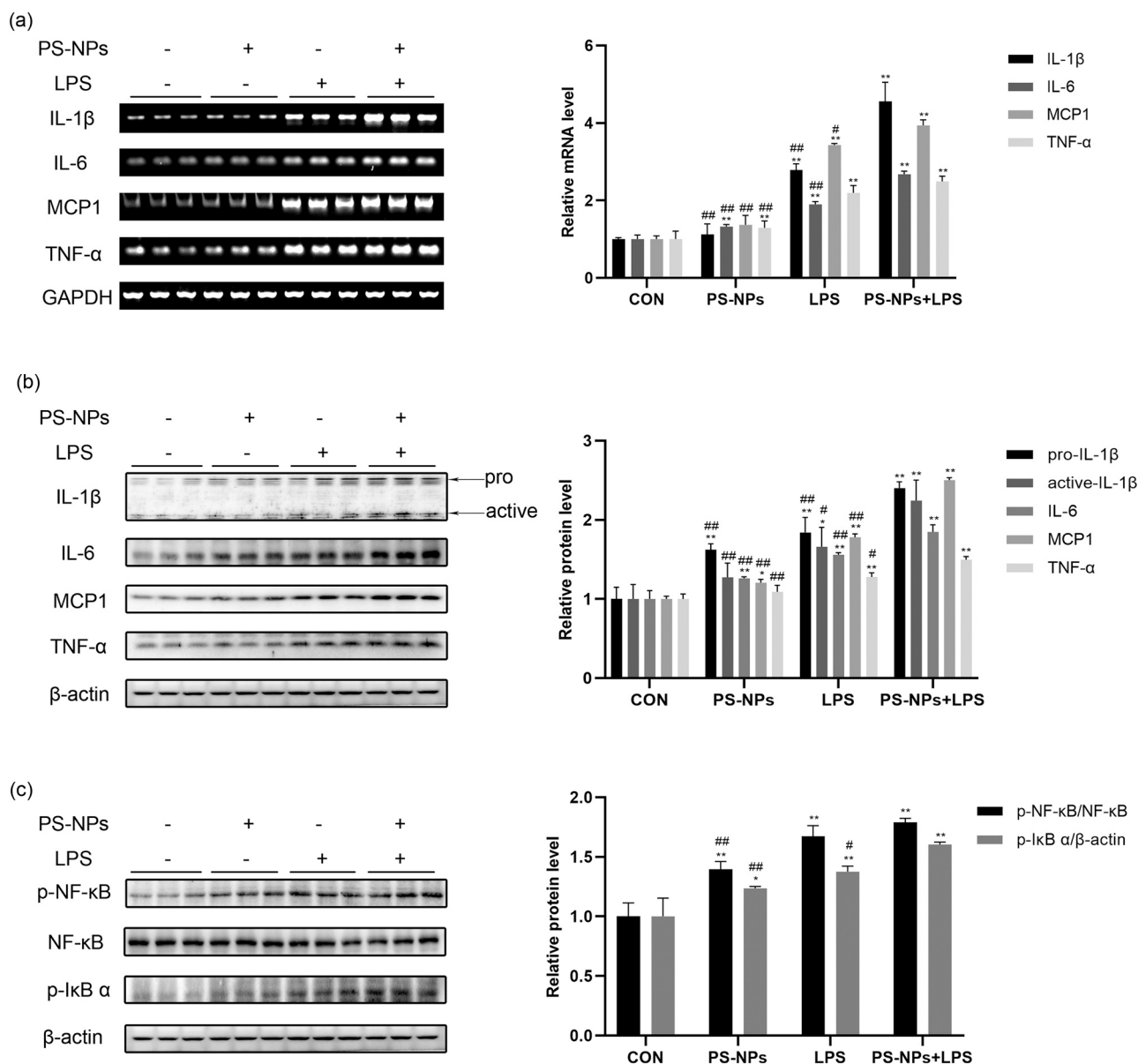


**Fig. 4.** The combined effect of PS-NPs and LPS on inflammatory factors expression in testes of mice. (a) The mRNA expressions of IL-1 $\beta$ , IL-6, MCP1 and TNF- $\alpha$  in testicular tissue of mice were detected by Semi-quantitative RT-PCR in the control, PS-NPs, LPS and PS-NPs + LPS group. GAPDH serves as an internal control for mRNA. The bar chart summarized the expression levels of mRNA IL-1 $\beta$ , IL-6, MCP1 and TNF- $\alpha$  in the PS-NPs, LPS, and PS-NPs + LPS group normalized to the control group. (b) The protein expressions of IL-1 $\beta$ , IL-6, MCP1 and TNF- $\alpha$  in testicular tissue of mice were detected by Western blot analysis in the control, PS-NPs, LPS and PS-NPs + LPS group.  $\beta$ -actin serves as an internal control for protein. The bar chart summarized the expression levels of protein pro-IL-1 $\beta$ , active-IL-1 $\beta$ , IL-6, MCP1 and TNF- $\alpha$  in the PS-NPs, LPS, and PS-NPs + LPS group normalized to the control group. Results were presented as the mean  $\pm$  SD ( $n = 6$ ). (c) Protein levels of p-NF- $\kappa$ B and TNF- $\alpha$  in the PS-NPs, LPS, and PS-NPs + LPS group normalized to the control group.  $\beta$ -actin and NF- $\kappa$ B serve as internal controls for p-I $\kappa$ B  $\alpha$  and p-NF- $\kappa$ B, respectively. The bar chart summarized the expression levels of protein p-I $\kappa$ B  $\alpha$  and p-NF- $\kappa$ B in the PS-NPs, LPS, and PS-NPs + LPS group normalized to the control group. Results were presented as the mean  $\pm$  SD ( $n = 6$ ). \* $p < 0.05$  and \*\* $p < 0.01$  vs the control group. # $p < 0.05$  and ## $p < 0.01$  vs the PS-NPs + LPS group.

significantly increased the activation of NF- $\kappa$ B. Therefore, NF- $\kappa$ B and HIF-1 $\alpha$  may play a crucial role in the sharp decrease in STAR mRNA expression levels induced by combined exposure to LPS and PS-NPs.

As LPS-induced inflammation in the testes of mice has been confirmed, LPS is often used for orchitis model in rats and mice (Metukuri et al., 2010; Sano et al., 2022). Recent studies have shown that after treatment with MPs or NPs, the expression of inflammatory factors in the testes of rodents significantly increase (Hou et al., 2021; Jin et al., 2021). Consistently, our results indicated that short-term exposure to PS-NPs or LPS increased the expression of inflammatory factors in the testes of mice including IL-1 $\beta$ , IL-6, TNF- $\alpha$ , and MCP1

mRNA and protein. Moreover, PS-NPs combined with LPS significantly enhanced the expression levels of these inflammatory factors mRNA and protein compared to PS-NPs or LPS alone. Oxidative stress is considered as an important factor in initiating inflammatory responses (Dutta et al., 2021). There are many mechanisms by which oxidative stress induces inflammatory cytokines expression in cells. One of these mechanisms is the activation of NF- $\kappa$ B. Oxidative stress has been proven to activate transcription factor NF- $\kappa$ B which can directly bind to the promoters of IL-1 $\beta$  (Cogswell et al., 1994), TNF- $\alpha$  (Trede et al., 1995), IL-6 (Mori et al., 1994) and MCP1 (You et al., 2014) to promote their transcription and increase the expression of inflammatory factors. As expected, our

findings showed that exposure to PS-NPs or LPS alone elevated the levels of phosphorylation of NF- $\kappa$ B and I $\kappa$ B  $\alpha$  which indicate NF- $\kappa$ B activation. Moreover, PS-NPs combined with LPS significantly elevated the phosphorylation levels of NF- $\kappa$ B and I $\kappa$ B  $\alpha$  compared to LPS alone. Consistent with this, the combination of PS-NPs and LPS significantly increased the expression of inflammatory factors compared to LPS treatment alone. Previous studies have shown that ROS generation induced by MPs/NPs exposure depends on the characterization of the MPs/NPs and the type of cell (Chen et al., 2023; Steckiewicz et al., 2022; Visalli et al., 2023). Therefore, the relationship between MPs/NPs exposure and ROS production are still undefined and more investigations are needed in the future. In this study, we found that PS-NPs exposure increased ROS production in mice testis. However, ROS generation induced by PS-NPs combined with LPS did not show a significantly stronger effect than those induced by LPS alone. This phenomenon may be due to LPS-induced ROS generation far exceeding that induced by PS-NPs, and LPS-induced ROS covers that induced by PS-NPs. In addition, the combination of PS-NPs and LPS induces NF- $\kappa$ B activation through other pathways besides oxidative stress.

However, there are some shortcomings in this study. The molecular mechanism by which the combined exposure to PS-NPs and LPS induce inflammation and reduce testosterone synthesis is not fully understood. Also, the potential reasons why the combined effect of PS-NPs and LPS on oxidative stress indicators does not significantly exceed that of LPS alone are worthy of investigation in the future. Furthermore, due to human long-term exposure to low-dose microplastics with different sizes, we will investigate the combined effects of long-term exposure to low-dose microplastics with different sizes and LPS on male reproductive function.

In summary, our results indicate that PS-NPs exacerbate the adverse effects of LPS on inflammation and testosterone biosynthesis in mouse testes. The combined effect of PS-NPs and LPS activated NF- $\kappa$ B and lead to an increase in the expression level of inflammatory factors in the testes of mice. In addition, activated NF- $\kappa$ B by PS-NPs and LPS inhibits the expression of StAR mRNA and protein, leading to a decrease in testosterone biosynthesis. Our study provides a valuable result on the combined effects of NPs and Gram negative bacteria on the male reproductive system.

#### CRedit authorship contribution statement

**Yanli Li:** Investigation; Methodology; Data curation; Formal analysis; Conceptualization; **Yingqi Liu:** Investigation; Methodology; Project administration; Validation; **Yanhong Chen:** Validation; **Chenjuan Yao:** Conceptualization; Project administration; **Shali Yu:** Methodology; **Jianhua Qu:** Methodology; Writing - review & editing; **Gang Chen:** Conceptualization; Supervision; Funding acquisition; Writing - original draft; Writing - review & editing; **Haiyan Wei:** Conceptualization; Supervision; Writing - original draft; Writing - review & editing.

#### Declaration of Competing Interest

The authors declare that they have no known competing financial interests or personal relationships that could have appeared to influence the work reported in this paper.

#### Data availability

Data will be made available on request.

#### Acknowledgments

This funding was provided by Nantong University (131500617260).

#### References

- Akang, E.N., Opuwari, C.S., Enyioma-Alozie, S., Mougala, L.W., Amatu, T.E., Wada, I., Ogbache, R.O., Ajayi, O.O., Aderonmu, M.M., Shote, O.B., Akinola, L.A., Ashiru, O. A., Henkel, R., 2023. Trends in semen parameters of infertile men in South Africa and Nigeria. *Sci. Rep.* 13 (1), 6819. <https://doi.org/10.1038/s41598-023-33648-4>.
- Alexander, C., Rietschel, E.T., 2001. Bacterial lipopolysaccharides and innate immunity. *J. Endotoxin Res.* 7 (3), 167–202 (DOI).
- Allen, J.A., Diemer, T., Janus, P., Hales, K.H., Hales, D.B., 2004. Bacterial endotoxin lipopolysaccharide and reactive oxygen species inhibit Leydig cell steroidogenesis via perturbation of mitochondria. *Endocrine* 25 (3), 265–275. <https://doi.org/10.1385/ENDO:25:3:265>.
- Amato-Lourenco, L.F., Carvalho-Oliveira, R., Junior, G.R., Dos Santos Galvao, L., Ando, R.A., Mauad, T., 2021. Presence of airborne microplastics in human lung tissue. *J. Hazard Mater.* 416, 126124 <https://doi.org/10.1016/j.jhazmat.2021.126124>.
- Auger, J., Kunstmann, J.M., Czyglik, F., Jouannet, P., 1995. Decline in semen quality among fertile men in Paris during the past 20 years. *N. Engl. J. Med.* 332 (5), 281–285. <https://doi.org/10.1056/NEJM199502023320501>.
- Bosmann, H.B., Hales, K.H., Li, X., Liu, Z., Stocco, D.M., Hales, D.B., 1996. Acute in vivo inhibition of testosterone by endotoxin parallels loss of steroidogenic acute regulatory (STAR) protein in Leydig cells. *Endocrinology* 137 (10), 4522–4525. <https://doi.org/10.1210/endo.137.10.8828518>.
- Cai, P., Wang, Y., Feng, N., Zou, H., Gu, J., Yuan, Y., Liu, X., Liu, Z., Bian, J., 2023. Polystyrene nanoplastics aggravate reproductive system damage in obese male mice by perturbation of the testis redox homeostasis. *Environ. Toxicol.* 38 (12), 2881–2893. DOI: 10.1002/tox.23923.
- Carlsen, E., Giwercman, A., Keiding, N., Skakkebaek, N.E., 1992. Evidence for decreasing quality of semen during past 50 years. *BMJ* 305 (6854), 609–613. <https://doi.org/10.1136/bmj.305.6854.609>.
- Chen, J., Xu, Z., Liu, Y., Mei, A., Wang, X., Shi, Q., 2023. Cellular absorption of polystyrene nanoplastics with different surface functionalization and the toxicity to RAW264.7 macrophage cells. *Ecotoxicol. Environ. Saf.* 252, 114574 <https://doi.org/10.1016/j.ecoenv.2023.114574>.
- Cogswell, J.P., Godlevski, M.M., Wisely, G.B., Clay, W.C., Leesnitzer, L.M., Ways, J.P., Gray, J.G., 1994. NF-kappa B regulates IL-1 beta transcription through a consensus NF-kappa B binding site and a nonconsensus CRE-like site. *J. Immunol.* 153 (2), 712–723. DOI: <https://www.ncbi.nlm.nih.gov/pubmed/8021507>.
- Curren, E., Leong, S.C.Y., 2019. Profiles of bacterial assemblages from microplastics of tropical coastal environments. *Sci. Total Environ.* 655, 313–320. <https://doi.org/10.1016/j.scitotenv.2018.11.250>.
- Dutta, S., Sengupta, P., Slama, P., Roychoudhury, S., 2021. Oxidative stress, testicular inflammatory pathways, and male reproduction. *Int. J. Mol. Sci.* 22 (18) <https://doi.org/10.3390/ijms221810043>.
- Farsimadan, M., Motamedifar, M., 2020. Bacterial infection of the male reproductive system causing infertility. *J. Reprod. Immunol.* 142, 103183 <https://doi.org/10.1016/j.jri.2020.103183>.
- Frede, S., Stockmann, C., Freitag, P., Fandrey, J., 2006. Bacterial lipopolysaccharide induces HIF-1 activation in human monocytes via p44/42 MAPK and NF-kappaB. *Biochem. J.* 396 (3), 517–527. DOI: 10.1042/bj20051839.
- Gao, L., Xiong, X., Chen, C., Luo, P., Li, J., Gao, X., Huang, L., Li, L., 2023. The male reproductive toxicity after nanoplastics and microplastics exposure: sperm quality and changes of different cells in testis. *Ecotoxicol. Environ. Saf.* 267, 115618 <https://doi.org/10.1016/j.ecoenv.2023.115618>.
- Hassine, M.B.H., Venditti, M., Rhouma, M.B., Minucci, S., Messaoudi, I., 2023. Combined effect of polystyrene microplastics and cadmium on rat blood-testis barrier integrity and sperm quality. *Environ. Sci. Pollut. Res. Int.* 30 (19), 56700–56712. <https://doi.org/10.1007/s11356-023-26429-z>.
- He, Y., Zou, L., Luo, W., Yi, Z., Yang, P., Yu, S., Liu, N., Ji, J., Guo, Y., Liu, P., He, X., Lv, Z., Huang, S., 2020. Heavy metal exposure, oxidative stress and semen quality: exploring associations and mediation effects in reproductive-aged men. *Chemosphere* 244, 125498. <https://doi.org/10.1016/j.chemosphere.2019.125498>.
- He, Y., Li, Z., Xu, T., Luo, D., Chi, Q., Zhang, Y., Li, S., 2022. Polystyrene nanoplastics deteriorate LPS-modulated duodenal permeability and inflammation in mice via ROS driven-NF- $\kappa$ B/NLRP3 pathway. *Chemosphere* 307 (Pt 1), 135662. <https://doi.org/10.1016/j.chemosphere.2022.135662>.
- Hernández-Sánchez, C., Pestana-Ríos, A., Villanova-Solano, A., Domínguez-Hernández, C., Díaz-Peña, C., Rodríguez-Álvarez, F.J., Lecuona, C., Arias, M., 2023. Bacterial colonization of microplastics at the beaches of an oceanic island, Tenerife, Canary Islands. *Int. J. Environ. Res. Public Health* 20 (5). <https://doi.org/10.3390/ijerph20053951>.
- Horvath, T., Tamminga, M., Liu, B., Sebode, M., Carambia, A., Fischer, L., Puschel, K., Huber, S., Fischer, E.K., 2022. Microplastics detected in cirrhotic liver tissue. *EBioMedicine* 82, 104147. <https://doi.org/10.1016/j.ebiom.2022.104147>.
- Hou, B., Wang, F., Liu, T., Wang, Z., 2021. Reproductive toxicity of polystyrene microplastics: in vivo experimental study on testicular toxicity in mice. *J. Hazard Mater.* 405, 124028 <https://doi.org/10.1016/j.jhazmat.2020.124028>.
- Ilechukwu, I., Ehigior, B.E., Ben, I.O., Okonkwo, C.J., Olorunfemi, O.S., Modo, U.E., Ilechukwu, C.E., Ohagwa, N.J., 2022. Chronic toxic effects of polystyrene microplastics on reproductive parameters of male rats. *e2022015-2022010 Environ. Anal. Health Toxicol.* 37 (2). <https://doi.org/10.5620/eah.2022015>.
- Irvine, S., Cawood, E., Richardson, D., MacDonald, E., Aitken, J., 1996. Evidence of deteriorating semen quality in the United Kingdom: birth cohort study in 577 men in Scotland over 11 years. *BMJ* 312 (7029), 467–471. <https://doi.org/10.1136/bmj.312.7029.467>.

- Jenner, L.C., Rotchell, J.M., Bennett, R.T., Cowen, M., Tentzeris, V., Sadofsky, L.R., 2022. Detection of microplastics in human lung tissue using muFTIR spectroscopy. *Sci. Total Environ.* 831, 154907 <https://doi.org/10.1016/j.scitotenv.2022.154907>.
- Jin, H., Ma, T., Sha, X., Liu, Z., Zhou, Y., Meng, X., Chen, Y., Han, X., Ding, J., 2021. Polystyrene microplastics induced male reproductive toxicity in mice. *J. Hazard Mater.* 401, 123430 <https://doi.org/10.1016/j.jhazmat.2020.123430>.
- Jin, H., Yan, M., Pan, C., Liu, Z., Sha, X., Jiang, C., Li, L., Pan, M., Li, D., Han, X., Ding, J., 2022. Chronic exposure to polystyrene microplastics induced male reproductive toxicity and decreased testosterone levels via the LH-mediated LHR/cAMP/PKA/StAR pathway. *Part Fibre Toxicol.* 19 (1), 13. <https://doi.org/10.1186/s12989-022-00453-2>.
- Junaid, M., Siddiqui, J.A., Sadaf, M., Liu, S., Wang, J., 2022. Enrichment and dissemination of bacterial pathogens by microplastics in the aquatic environment. *Sci. Total Environ.* 830, 154720 <https://doi.org/10.1016/j.scitotenv.2022.154720>.
- Knapke, E.T., Magalhaes, D.P., Dalvie, M.A., Mandrioli, D., Perry, M.J., 2022. Environmental and occupational pesticide exposure and human sperm parameters: a navigation guide review. *Toxicology* 465, 153017. <https://doi.org/10.1016/j.tox.2021.153017>.
- Leslie, H.A., van Velzen, M.J.M., Brandsma, S.H., Vethaak, A.D., Garcia-Vallejo, J.J., Lamoree, M.H., 2022. Discovery and quantification of plastic particle pollution in human blood. *Environ. Int.* 163, 107199 <https://doi.org/10.1016/j.envint.2022.107199>.
- Levine, H., Jorgensen, N., Martino-Andrade, A., Mendiola, J., Weksler-Derri, D., Mindlis, I., Pinotti, R., Swan, S.H., 2017. Temporal trends in sperm count: a systematic review and meta-regression analysis. *Hum. Reprod.* Update 23 (6), 646–659. <https://doi.org/10.1093/humupd/dmx022>.
- Li, M.W., Mruk, D.D., Lee, W.M., Cheng, C.Y., 2009. Disruption of the blood-testis barrier integrity by bisphenol A in vitro: is this a suitable model for studying blood-testis barrier dynamics? *Int. J. Biochem. Cell Biol.* 41 (11), 2302–2314. <https://doi.org/10.1016/j.biocel.2009.05.016>.
- Li, S., Wang, Q., Yu, H., Yang, L., Sun, Y., Xu, N., Wang, N., Lei, Z., Hou, J., Jin, Y., Zhang, H., Li, L., Xu, F., Zhang, L., 2021. Polystyrene microplastics induce blood-testis barrier disruption regulated by the MAPK-Nrf2 signaling pathway in rats. *Environ. Sci. Pollut. Res. Int.* 28 (35), 47921–47931. <https://doi.org/10.1007/s11356-021-13911-9>.
- Li, Z., Xu, T., Peng, L., Tang, X., Chi, Q., Li, M., Li, S., 2023. Polystyrene nanoplastics aggravates lipopolysaccharide-induced apoptosis in mouse kidney cells by regulating IRE1/XBP1 endoplasmic reticulum stress pathway via oxidative stress. *J. Cell Physiol.* 238 (1), 151–164. DOI: 10.1002/jcp.30913.
- Lin, P., Tong, X., Yue, F., Qianru, C., Xinyu, T., Zhe, L., Zhikun, B., Shu, L., 2022. Polystyrene nanoplastics exacerbate lipopolysaccharide-induced myocardial fibrosis and autophagy in mice via ROS/TGF- $\beta$ 1/Smad. *Toxicology* 480, 153338. <https://doi.org/10.1016/j.tox.2022.153338>.
- Ma, S., Wang, L., Li, S., Zhao, S., Li, F., Li, X., 2023. Transcriptome and proteome analyses reveal the mechanisms involved in polystyrene nanoplastics disrupt spermatogenesis in mice. *Environ. Pollut.* 342, 123086 <https://doi.org/10.1016/j.envpol.2023.123086>.
- Mackern-Oberti, J.P., Motrich, R.D., Bresler, M.L., Sanchez, L.R., Cuffini, C., Rivero, V.E., 2013. *Chlamydia trachomatis* infection of the male genital tract: an update. *J. Reprod. Immunol.* 100 (1), 37–53. <https://doi.org/10.1016/j.jri.2013.05.002>.
- Manouchehri, A., Shokri, S., Pirhadi, M., Karimi, M., Abbaszadeh, S., Mirzaei, G., Bahmani, M., 2022. The effects of toxic heavy metals lead, cadmium and copper on the epidemiology of male and female infertility. *JBRA Assist Reprod.* 26 (4), 627–630. <https://doi.org/10.5935/1518-0557.20220013>.
- Metukuri, M.R., Reddy, C.M., Reddy, P.R., Reddanna, P., 2010. Bacterial LPS-mediated acute inflammation-induced spermatogenic failure in rats: role of stress response proteins and mitochondrial dysfunction. *Inflammation* 33 (4), 235–243. <https://doi.org/10.1007/s10753-009-9177-4>.
- Montano, L., Giorgini, E., Notarstefano, V., Notari, T., Ricciardi, M., Piscopo, M., Motta, O., 2023. Raman Microspectroscopy evidence of microplastics in human semen. *Sci. Total Environ.* 901, 165922 <https://doi.org/10.1016/j.scitotenv.2023.165922>.
- Mori, N., Shirakawa, F., Shimizu, H., Murakami, S., Oda, S., Yamamoto, K., Eto, S., 1994. Transcriptional regulation of the human interleukin-6 gene promoter in human T-cell leukemia virus type I-infected T-cell lines: evidence for the involvement of NF-kappa B. *Blood* 84 (9), 2904–2911. DOI: <https://www.ncbi.nlm.nih.gov/pubmed/7949164>.
- Nelson, C.M., Bunge, R.G., 1974. Semen analysis: evidence for changing parameters of male fertility potential. *Fertil. Steril.* 25 (6), 503–507. [https://doi.org/10.1016/s0015-0282\(16\)40454-1](https://doi.org/10.1016/s0015-0282(16)40454-1).
- Nikolic, S., Gazdic-Jankovic, M., Rosic, G., Miletic-Kovacevic, M., Jovicic, N., Nestorovic, N., Stojkovic, P., Filipovic, N., Milosevic-Djordjevic, O., Selakovic, D., Zivanovic, M., Seklic, D., Milivojevic, N., Markovic, A., Seist, R., Vasiljic, S., Stankovic, K.M., Stojkovic, M., Ljubic, B., 2022. Orally administered fluorescent nanosized polystyrene particles affect cell viability, hormonal and inflammatory profile, and behavior in treated mice. *Environ. Pollut.* 305, 119206 <https://doi.org/10.1016/j.envpol.2022.119206>.
- O'Brien, S., Rauter, C., Ribeiro, F., Okoffo, E.D., Burrows, S.D., O'Brien, J.W., Wang, X., Wright, S.L., Thomas, K.V., 2023. There's something in the air: a review of sources, prevalence and behaviour of microplastics in the atmosphere. *Sci. Total Environ.* 874, 162193 <https://doi.org/10.1016/j.scitotenv.2023.162193>.
- Okonofua, F.E., Ntoimo, L.F.C., Omonkhua, A., Ayodeji, O., Olafusi, C., Unuabonah, E., Ohenhen, V., 2022. Causes and risk factors for male infertility: a scoping review of published studies. *Int. J. Gen. Med.* 15, 5985–5997. <https://doi.org/10.2147/IJGM.S363959>.
- Palladino, M.A., Fasano, G.A., Patel, D., Dugan, C., London, M., 2018. Effects of lipopolysaccharide-induced inflammation on hypoxia and inflammatory gene expression pathways of the rat testis. *Basic Clin. Androl.* 28, 14. <https://doi.org/10.1186/s12610-018-0079-x>.
- Peretz, J., Flaws, J.A., 2013. Bisphenol A down-regulates rate-limiting Cyp11a1 to acutely inhibit steroidogenesis in cultured mouse antral follicles. *Toxicol. Appl. Pharm.* 271 (2), 249–256. <https://doi.org/10.1016/j.taap.2013.04.028>.
- Ragusa, A., Svelato, A., Santacrose, C., Catalano, P., Notarstefano, V., Carnevali, O., Papa, F., Rongioletti, M.C.A., Baiocco, F., Draghi, S., D'Amore, E., Rinaldo, D., Matta, M., Giorgini, E., 2021. Plasticenta: first evidence of microplastics in human placenta. *Environ. Int.* 146, 106274 <https://doi.org/10.1016/j.envint.2020.106274>.
- Ramsperger, A., Bergamaschi, E., Panizzolo, M., Fenoglio, I., Barbero, F., Peters, R., Undas, A., Purker, S., Giese, B., Lalyer, C.R., Tamargo, A., Moreno-Arribas, M.V., Grossart, H.P., Kuhnel, D., Dietrich, J., Paulsen, F., Afanou, A.K., Zienoldind-Narui, S., Eriksen Hammer, S., Kringlen Ervik, T., Graff, P., Brinckmann, B.C., Nordby, K.C., Wallin, H., Nassi, M., Benetti, F., Zanella, M., Brehm, J., Kress, H., Loder, M.G.J., Laforsch, C., 2023. Nano- and microplastics: a comprehensive review on their exposure routes, translocation, and fate in humans. *NanoImpact* 29, 100441. <https://doi.org/10.1016/j.impact.2022.100441>.
- Rokade, S., Upadhyay, M., Bhat, D.S., Subhedar, N., Yajnik, C.S., Ghose, A., Rath, S., Bal, V., 2021. Transient systemic inflammation in adult male mice results in underweight progeny. *Am. J. Reprod. Immunol.* 86 (1), e13401. DOI: 10.1111/aji.13401.
- Rotchell, J.M., Jenner, L.C., Chapman, E., Bennett, R.T., Bolanle, I.O., Loubani, M., Sadofsky, L., Palmer, T.M., 2023. Detection of microplastics in human saphenous vein tissue using muFTIR: a pilot study. *PLoS One* 18 (2), e0280594. <https://doi.org/10.1371/journal.pone.0280594>.
- Ryan, L., Daly, P., Cullen, I., Doyle, M., 2018. Epididymo-orchitis caused by enteric organisms in men > 35 years old: beyond fluoroquinolones. *Eur. J. Clin. Microbiol. Infect. Dis.* 37 (6), 1001–1008. <https://doi.org/10.1007/s10096-018-3212-z>.
- Sadasivam, M., Ramachandirin, B., Ayyanar, A., Prahalathan, C., 2014. Bacterial lipopolysaccharide differentially modulates steroidogenic enzymes gene expressions in the brain and testis in rats. *Neurosci. Res.* 83, 81–88. <https://doi.org/10.1016/j.neures.2014.02.011>.
- Sano, M., Komiya, H., Shinoda, R., Ozawa, R., Watanabe, H., Karasawa, T., Takahashi, M., Torii, Y., Iwata, H., Kuwayama, T., Shirasuna, K., 2022. NLRP3 inflammasome is involved in testicular inflammation induced by lipopolysaccharide in mice. *Am. J. Reprod. Immunol.* 87 (4), e13527. DOI: 10.1111/aji.13527.
- Senathirajah, K., Attwood, S., Bhagwat, G., Carbery, M., Wilson, S., Palanisami, T., 2021. Estimation of the mass of microplastics ingested - A pivotal first step towards human health risk assessment. *J. Hazard Mater.* 404 (Pt B), 124004 <https://doi.org/10.1016/j.jhazmat.2020.124004>.
- Sewwandi, M., Wijesekara, H., Rajapaksha, A.U., Soysa, S., Vithanage, M., 2023. Microplastics and plastics-associated contaminants in food and beverages; global trends, concentrations, and human exposure. *Environ. Pollut.* 317, 120747 <https://doi.org/10.1016/j.envpol.2022.120747>.
- Shen, P., Ji, S., Li, X., Yang, Q., Xu, B., Wong, C.K.C., Wang, L., Li, L., 2022. LPS-induced systemic inflammation caused mPOA-FSH/LH disturbance and impaired testicular function. *Front. Endocrinol. (Lausanne)* 13, 886085. <https://doi.org/10.3389/fendo.2022.886085>.
- Smith, L.B., Walker, W.H., 2014. The regulation of spermatogenesis by androgens. *Semin. Cell Dev. Biol.* 30, 2–13. <https://doi.org/10.1016/j.semedb.2014.02.012>.
- Steckiewicz, K.P., Adamska, A., Narajczyk, M., Megiel, E., Inkielewicz-Stepniak, I., 2022. Fluoride enhances polystyrene nanoparticles cytotoxicity in colonocytes in vitro model. *Chem. Biol. Inter.* 367, 110169 <https://doi.org/10.1016/j.cbi.2022.110169>.
- Sui, A., Yao, C., Chen, Y., Li, Y., Yu, S., Qu, J., Wei, H., Tang, J., Chen, G., 2023. Polystyrene nanoplastics inhibit StAR expression by activating HIF-1 $\alpha$  via ERK1/2 MAPK and AKT pathways in TM3 Leydig cells and testicular tissues of mice. *Food Chem. Toxicol.* 173, 113634 <https://doi.org/10.1016/j.fct.2023.113634>.
- Sun, Z., Wen, Y., Zhang, F., Fu, Z., Yuan, Y., Kuang, H., Kuang, X., Huang, J., Zheng, L., Zhang, D., 2023. Exposure to nanoplastics induces mitochondrial impairment and cytomembrane destruction in Leydig cells. *Ecotoxicol. Environ. Saf.* 255, 114796 <https://doi.org/10.1016/j.ecoenv.2023.114796>.
- Sziva, R.E., Ács, J., Tőkés, A.M., Korsós-Novák, Á., Nádas, G.L., Ács, N., Horváth, P.G., Szabó, A., Ke, H., Horváth, E.M., Kopa, Z., Várbíró, S., 2022. Accurate quantitative histomorphometric-mathematical image analysis methodology of rodent testicular tissue and its possible future research perspectives in andrology and reproductive medicine. *Life* 12 (2). <https://doi.org/10.3390/life12020189>.
- Tang, X., Fan, X., Xu, T., He, Y., Chi, Q., Li, Z., Li, S., 2022. Polystyrene nanoplastics exacerbated lipopolysaccharide-induced necroptosis and inflammation via the ROS/MAPK pathway in mice spleen. *Environ. Toxicol.* 37 (10), 2552–2565. DOI: 10.1002/tox.23618.
- Trede, N.S., Tsytsykova, A.V., Chatila, T., Goldfeld, A.E., Geha, R.S., 1995. Transcriptional activation of the human TNF- $\alpha$  promoter by superantigen in human monocytic cells: role of NF-kappa B. *J. Immunol.* 155 (2), 902–908. DOI: <https://www.ncbi.nlm.nih.gov/pubmed/7608567>.
- Visalli, G., Laganà, A., Facciola, A., Iaconis, A., Curcio, J., Pollino, S., Celesti, C., Scalese, S., Libertino, S., Iannazzo, D., Di Pietro, A., 2023. Enhancement of biological effects of oxidised nano- and microplastics in human professional phagocytes. *Environ. Toxicol. Pharm.* 99, 104086 <https://doi.org/10.1016/j.etap.2023.104086>.
- Wei, Y., Zhou, Y., Long, C., Wu, H., Hong, Y., Fu, Y., Wang, J., Wu, Y., Shen, L., Wei, G., 2021. Polystyrene microplastics disrupt the blood-testis barrier integrity through ROS-Mediated imbalance of mTORC1 and mTORC2. *Environ. Pollut.* 289, 117904 <https://doi.org/10.1016/j.envpol.2021.117904>.
- Xu, W., Yuan, Y., Tian, Y., Cheng, C., Chen, Y., Zeng, L., Yuan, Y., Li, D., Zheng, L., Luo, T., 2023. Oral exposure to polystyrene nanoplastics reduced male fertility and

- even caused male infertility by inducing testicular and sperm toxicities in mice. *J. Hazard Mater.* 454, 131470 <https://doi.org/10.1016/j.jhazmat.2023.131470>.
- You, J.J., Yang, C.H., Yang, C.M., Chen, M.S., 2014. Cyr61 induces the expression of monocyte chemoattractant protein-1 via the integrin  $\alpha$ 5 $\beta$ 1, FAK, PI3K/Akt, and NF- $\kappa$ B pathways in retinal vascular endothelial cells. *Cell Signal* 26 (1), 133–140. <https://doi.org/10.1016/j.cellsig.2013.08.026>.
- Zhang, Q., Xu, E.G., Li, J., Chen, Q., Ma, L., Zeng, E.Y., Shi, H., 2020. A review of microplastics in table salt, drinking water, and air: direct human exposure. *Environ. Sci. Technol.* 54 (7), 3740–3751. <https://doi.org/10.1021/acs.est.9b04535>.
- Zhao, Q., Zhu, L., Weng, J., Jin, Z., Cao, Y., Jiang, H., Zhang, Z., 2023. Detection and characterization of microplastics in the human testis and semen. *Sci. Total Environ.* 877, 162713 <https://doi.org/10.1016/j.scitotenv.2023.162713>.
- Zhou, N., Cui, Z., Yang, S., Han, X., Chen, G., Zhou, Z., Zhai, C., Ma, M., Li, L., Cai, M., Li, Y., Ao, L., Shu, W., Liu, J., Cao, J., 2014. Air pollution and decreased semen quality: a comparative study of Chongqing urban and rural areas. *Environ. Pollut.* 187, 145–152. <https://doi.org/10.1016/j.envpol.2013.12.030>.